Journal of Power Sources 206 (2012) 161–170

Contents lists available at SciVerse ScienceDirect

Journal of Power Sources

journal homepage: www.elsevier.com/locate/jpowsour

Impact of gas stoichiometry on water management and fuel cell performance of a sulfonated Poly(Ether Ether Ketone) membrane

P.M. Legrand [a], A. Morin [b,*], V.H. Mareau [a], L. Gonon [a]

[a] Structures et Propriétés d'Architectures Moléculaires, UMR 5819 (CEA-CNRS-UJF), INAC/SPrAM, CEA-Grenoble, 38054 Grenoble Cedex 9, France
[b] CEA DRT/Liten/DEHT/LCPEM, CEA-Grenoble, 17 rue des Martyrs, F-38054 Grenoble Cedex 9, France

ARTICLE INFO

Article history:
Received 25 July 2011
Received in revised form 4 January 2012
Accepted 6 January 2012
Available online 20 January 2012

Keywords:
PEMFC
sPEEK
Nafion
Gas stoichiometry
Water management
Performances

ABSTRACT

Fuel cell tests have been performed on sulfonated Poly(Ether Ether Ketone) (sPEEK) membranes using dry gases. Impact of gas stoichiometry on performance evolution and membrane–electrodes assembly's water distribution optimization (water management) was studied. During the tests, output voltage evolution was recorded as well as impedance spectra, polarization curves and water amount collected at both sides.

Fuel cell performances were observed to be influenced by water management which depends on both operating conditions and membrane intrinsic properties. Increasing either hydrogen or oxygen stoichiometry leads to a decrease of performance. This effect was more pronounced for hydrogen increase (anode). This has been ascribed to a global drying of the membrane along with the appearance of a heterogeneous hydration both through the MEA and along the gas channels.

Cell performance characterization during the membrane lifespan was mainly based on Electrochemical Impedance Spectroscopy measurements and showed that water distribution heterogeneity increased with operating time for sPEEK membrane, leading to a drop of performance. This was mainly ascribed to the drying of the gas inlet and the increased hydration at the gas outlet. These behaviours were not observed for the better performing Nafion, which underlines the impact of membrane water transport properties on fuel cell performance.

1. Introduction

In the next decades fuel cells will play a major role in clean power production as a secure and sustainable energy [1]. Researches on various fuel cell technologies using different electrolytes, like alkaline fuel cells (AFC), solid oxide fuel cells (SOFC), proton exchange membrane fuel cells (PEMFC), have reached a high level of development. This diversification offers numerous applications in non polluting systems, from automotive to stationary and portable applications. Their advantages are their high efficiency, the absence of noise pollution and first of all their "zero emission" potential. However, fuel cells as clean energy delivery systems still have to deal with durability and cost issues [2,3].

For PEMFC, the membrane electrodes assembly (MEA) is the active core of the fuel cell in which the electrochemical reactions take place. It consists of a polymer membrane sandwiched between two electrodes (anode and cathode). Hydrogen is supplied at the anode where it is oxidized and oxygen is supplied at the cathode side where it is reduced. The main role of the membrane is to carry protons from the anode to the cathode (where water is produced). It must be at the same time an electrical insulator and a gas separator. State of the art membranes usually consist of a hydrophobic polymer backbone with acid groups (for proton conductivity) distributed either directly on the backbone, or on side chains. As the proton conductivity strongly depends on the water content of the polymer [4], water management is essential for the enhancement of fuel cell performance. During fuel cell operation a lot of water being produced at the cathode side, a high water concentration gradient appears across the membrane and water diffuses from cathode to anode due to capillary forces. This is called back-diffusion [5]. On the other hand, water is dragged by the moving protons from anode to cathode, the so-called electro osmosis drag [6]. These phenomena are illustrated on Fig. 1. Water management is a key point for PEMFC when trying to improve both its performance and durability. For a given membrane a better water management can be achieved by choosing the proper operating parameters.

Abbreviations: AFC, alkaline fuel cells; BPSH, Bi Phenyl Sulfone H-form; EIS, Electrochemical Impedance Spectroscopy; MEA, membrane–electrodes assembly; OCV, Open Circuit Voltage; PEMFC, proton exchange membrane fuel cell; PVDF, PolyVinyliDene Fluoride; RH, relative humidity; R_{ohm}, ohmic resistance; R_{elec}, electrodes resistance; SOFC, solid oxide fuel cell; sPEEK, sulfonated Poly(Ether Ether Ketone).

* Corresponding author. Tel.: +33 4 38 78 59 86; fax: +33 4 38 78 94 63.
E-mail address: arnaud.morin@cea.fr (A. Morin).

0378-7753/$ – see front matter © 2012 Elsevier B.V. All rights reserved.
doi:10.1016/j.jpowsour.2012.01.102

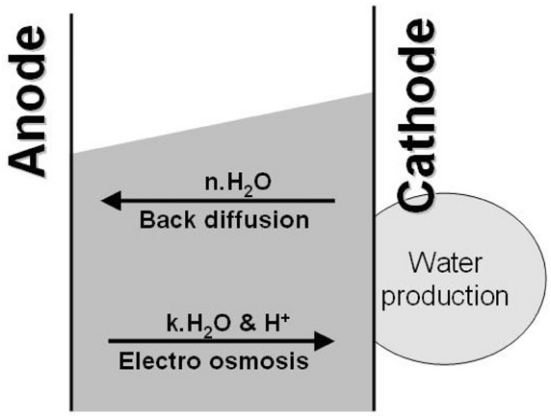

Fig. 1. Schematic representation of water flows across membrane in a PEMFC.

For PEMFC, the reference membrane is Nafion, a perfluorosulfonic polymer. However, despite its good properties up to 80 °C, a loss of its mechanical properties at higher temperatures prevents future development aiming to increase fuel cell efficiency through a working temperature increase. To overcome this issue, researches have been focused on sulfonated aromatic polymers. Despite a lower conductivity at low relative humidity (RH) [7,8] and a limited lifetime attributed to a chemical degradation [9,10], sulfonated aromatic polymers are particularly promising. They offer better thermo-mechanical [11] and permeation [12,13] properties in addition to a lower cost [14,15].

In order to improve both performance and durability, it is possible to adjust many parameters like operating temperature, gas relative humidity, pressure and flow (generally referred as gas stoichiometry). Many studies about operating conditions impact on fuel cell efficiency have been already performed for Nafion [16–18] but this type of information is still very scarce for aromatic polymers. Alberti et al. [7] showed that both Nafion 117 and sulfonated Poly(Ether Ether Ketone) (sPEEK) membranes can exhibit good proton conductivity (up to 50 mS cm^{-1}) at high temperature (150 °C) and RH (75%). Jiang et al. [19] studied for sPEEK membrane the impact of current density, temperature and relative humidity on water management and thus fuel cell performance. They showed that at high current density, back-diffusion effect is not sufficient to counter electro osmosis drag, leading to a drying of the anode side, and therefore a higher membrane resistance and a loss of the fuel cell performance. This phenomenon decreases when the temperature is increased, as water diffusion coefficient increases with temperature. They also found that fuel cell performance decreases for low gas RH as the ionomer membrane dries out.

Our study is focused on the impact of gas stoichiometry on water management and hence fuel cell performance of sPEEK membrane when using dry gases. Water management is studied by collecting water on anode and cathode sides. Performance is evaluated through polarization curves recording. Their evolution at a fixed current density is analysed thanks to Electrochemical Impedance Spectroscopy (EIS) which gives information about hydration homogeneity on the whole active surface area. sPEEK results are then compared to those obtained for Nafion for two operating conditions i.e. for the best and the worst conditions found for sPEEK.

2. Experimental

2.1. Membranes and MEAs

We studied sPEEK E-750 from Fumatech and Nafion NRE 212 from DuPont. The thickness of both membranes was about 50 μm and their ionic exchange capacity (IEC) was respectively of 1.35 and 0.9 mequiv. g^{-1}. Membranes were pretreated before use: sPEEK was immersed at room temperature in H_2SO_4 1 M for 4 h and then washed 3 times in ultrapure water at room temperature; Nafion NRE 212 was immersed at 70 °C in HCl 1 M for 2 h and then washed 3 times in ultrapure water at 70 °C.

Table 1
Gas flow rates corresponding to the chosen stoichiometry at 0.4 A cm^{-2}.

Stoichiometry anode/cathode	H_2 flow rate (N ml min^{-1})[a]	O_2 flow rate (N ml min^{-1})
1.5/1.5	21	11
1.5/3	21	22
3/1.5	42	11
3/3	42	22

[a] N ml min^{-1} stands for normalized flow rate to standard conditions of pressure and temperature.

MEAs were assembled by hot pressing the membrane between two electrodes "E-TEK ELAT® GDE LT120EW" (Pt loading 0.5 mg cm^{-2}) in two steps: 1 MPa for 3 min 30 s then 6 MPa for 3 min 30 s at 135 °C. After being hot-pressed, the MEA was placed into 5 cm^2 single cell fixtures. Airtightness was insured using 270 μm thick Viton gaskets. The single cell was made of two graphite monopolar plates with a single machined serpentine channel. Both channels width and depth are 1.4 mm whereas ribs width is 0.8 mm.

2.2. Fuel cell tests

In situ tests were carried out on a Bio-Logic FCT 150-S commercial bench. Cell temperature, current density as well as gas flow, pressure and relative humidity both at the cathode and anode sides were controlled. Two types of tests were performed: "ageing tests" where fuel cell performance of sPEEK and Nafion membranes (and associated MEAs) were studied; and "hydration tests" where drying was simulated at one or both electrode sides on sPEEK.

2.2.1. "Ageing tests"

In situ ageing tests were performed at 80 °C. Dry hydrogen and oxygen, absolute pressure of 2 bar, were applied in co-flow configuration (with H_2 and O_2 inlets both at the bottom of the fuel cell). Usually use of dry gases in fuel cells is motivated by the increased simplicity and efficiency of the system. In this study dry gases are provided to the fuel cell mainly to amplify the impact of operating conditions on the MEA hydration, enhancing the difference of gas hydration between the inlet and outlet. MEA is therefore drier near the gas inlet, whereas it is more hydrated near the outlet due to water production. The co-flow configuration also amplifies this phenomenon. Current density was constant and set to 0.4 A cm^{-2}.

To study their impact on performance, gas flows were controlled to keep a constant stoichiometry of either 1.5 or 3. In the following, a stoichiometry of 1.5 or 3 will mean that an excess of 50% or 200% of gases is provided to the fuel cell, compared to what needed to produce the collected current. Indeed, a stoichiometry set to 1 leads to flooding as all gases are consumed and therefore cannot push away produced water. It would be more correct to speak of gas flows instead of stoichiometry, but this misuse of language is convenient considering the overall reaction of the fuel cell $H_2 + (1/2)O_2 \rightarrow H_2O$ and is commonly used in the literature [18,20,21].

Correspondences between applied stoichiometries and gas flow rates at 0.4 A cm^{-2} are indicated in Table 1:

2.2.2. "Hydration tests"

"Hydration tests" were performed at 80 °C. Hydrogen and oxygen, absolute pressure of 2 bar, were applied in co-flow configuration with H_2 and O_2 inlets both at the bottom of the fuel cell. Current density was varied from 0.1 to 1.0 A cm^{-2} in order to vary both the amount of produced water and the electro-osmosis dragging force. Gas flow rates and RH were chosen in order to induce drying at one or both electrode sides. For all configurations,

gas flow rates are set to 666 N ml min^{-1}, corresponding to the maximum value of the hydrogen flow authorized by the bench. Gas flows were fixed and were the same at both sides in order to obtain the same pressure drop between gas inlet and outlet in each compartment of the symmetric cell. Our objective was to obtain as homogeneous water distribution within the cell as possible. H_2/O_2 resulting stoichiometries were 189/377 at 0.1 A cm^{-2}, 94/189 at 0.2 A cm^{-2}, 47/94 at 0.4 A cm^{-2}, etc.

Dry gases were directly provided to the fuel cell. For hydrated gases we used a bubbler chamber filled with water. RH of gases were controlled between 9 and 100% by adjusting temperature of the bubble chamber (between 30 and 85 °C). In the latter case, bubble chamber temperature was set higher than fuel cell temperature in order to be sure to have 100%RH (presence of liquid water in the fuel cell).

Impact of drying was studied by decreasing RH value from 100% to 0% on one electrode side. For symmetric drying (both electrode sides), RH values were decreased down to 9%RH. It was impossible to work at 0%RH on both sides with this high gas flow rate, as it would have totally dried the MEA.

At the inlet, oxygen partial pressure was adjusted in order to have a total pressure of 2 bar. $P_{O_2} = 1.53$ bar at 100%RH, 1.96 bar at 9%RH and 2 bar at 0%RH.

For 100%RH, gases that went through a bubble chamber filled with hot water (85 °C) were then carried to the cell through high temperature (120 °C) lines. It is difficult to tell if water was or not condensed between the bubble chamber and the cell. It is however known that cold points can be found inside the bench. Therefore we know for sure that liquid water existed inside the cell and gases were at 100%RH. As gas flow rates were very high, liquid water was easily removed and flooding was avoided.

In the 9/9%RH configuration (drying both electrode sides), calculations show that RH at the gas outlets at 0.4 A cm^{-2} cannot exceed 22% even with a water net flow from an electrode side to another. Calculations confirm that flooding is naturally avoided in this case.

For both "ageing" and "hydration" tests, the cell was started the same way. The cell was first heated up to 60 °C and in parallel the current density was increased until 0.2 A cm^{-2}. After about 12 h (needed to reach performance stabilisation), temperature and current density were increased respectively up to 80 °C and 0.4 A cm^{-2}. Then the voltage output was recorded as well as polarization curves followed by impedance spectroscopy every 48 h. Collected water was quantified for each electrode side at regular time interval (about 48 h) during fuel cell operation. The fuel cell was automatically stopped when the voltage dropped under 0.1 V (fuel cell breakdown).

2.3. Polarization curves

Fuel cell systems were characterized through the response of voltage to current impulse. Polarization curves were recorded with a current scan ranging from Open Circuit Voltage (OCV) to 0.6 A cm^{-2}. The scanning rate was 2 mA cm^{-2} s^{-1} between 0 and 0.2 A cm^{-2}, and 8 mA cm^{-2} s^{-1} between 0.2 and 0.6 A cm^{-2}.

2.4. Impedance spectroscopy

The Electrochemical Impedance Spectroscopy (EIS) technique in the galvanodynamic mode consists in applying a small sinusoidal current perturbation (of known amplitude and frequency) to the cell while measuring the amplitude and phase of the resulting voltage as a function of frequency. On one hand, the ratio between voltage/current amplitudes defines the impedance modulus $|Z|$ and on the other hand the phase difference between voltage and current gives access to real and imaginary parts of complex impedance Z.

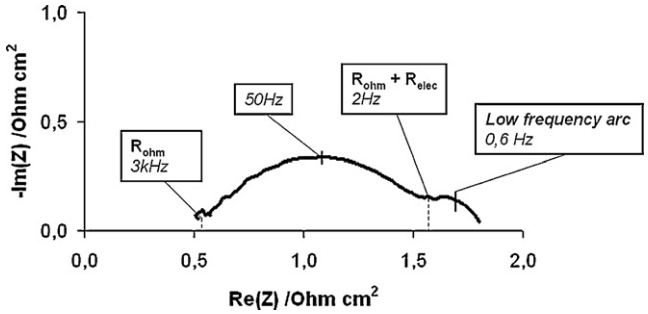

Fig. 2. Measurement of R_{ohm} and R_{elec} on a Nyquist diagram obtained during fuel cell operation.

During fuel cell "ageing tests", data was recorded using "FC Lab" software. EIS was conducted at 0.4 A cm^{-2} and by applying a 10 mA cm^{-2} amplitude current density with a frequency range from 10 kHz to 1 Hz. During "hydration tests", EIS measurements were carried out using a *Biologic* VSP galvanostat with a 20A/2V *VMP2B* booster and the "EC Lab" software. EIS measurements were performed at different current densities (from 0.1 to 1.0 mA cm^{-2}) by applying a 10 mA cm^{-2} amplitude current density with a frequency range from 100 kHz to 0.1 Hz.

In each case, real and imaginary parts of the complex impedance (Z) were obtained for different frequencies and plotted in a Nyquist diagram. Impedance spectra were analysed by considering mainly two contributions (Fig. 2) that are ascribed to the ohmic resistance R_{ohm} and electrode losses R_{elec}.

The ohmic resistance (R_{ohm}) corresponds to the real part of the impedance value at high frequency for which the imaginary part of impedance is equal to zero. It represents the proton resistance in the ionomer (membrane) and the various resistances such as electronic resistance for each electrode (about 10 mΩ cm^2 [22]) and contact resistance between monopolar plates and electrodes (about 5 mΩ cm^2 [23]). So, the non ionic contribution of the total ohmic specific resistance is around 30 mΩ cm^2 which represents a resistance of 6 mΩ with our cell design. These latter contributions are sometimes negligible compared to the ionic resistivity [24] but are significant in our study, in particular with the use of Nafion membrane.

Assuming a homogeneous hydration of the ionomer, membrane conductivity can be estimated:

$$\sigma = \frac{l}{R_{mem} \cdot S} \quad (1)$$

where σ is the conductivity, l is the distance between electrodes, $R_{mem} = R_{ohm} - 6\,(\text{m}\Omega)$ is the membrane resistance and S is the active surface.

In some cases the Nyquist plot does not cross the real axis even at 10 kHz and in the same time the spectra is noisy. In that case, the value of R_{ohm} is extrapolated by fitting the Nyquist diagram for high frequencies.

At low frequency values, the polarization resistance other than ohmic is ascribed to the phenomena occurring within the electrodes (R_{elec}) and more precisely to:

- Charge transfer which refers to the exchange of electrons from the reactant adsorbed onto the surface of the catalyst to the catalyst itself [25,26].
- Mass transport which corresponds to the diffusion of reactants towards the catalytic sites [25,26].
- Protons migration towards the catalytic sites [27].

R_{elec} is deduced from the total polarization resistance ($R_{ohm} + R_{elec}$) which is read at the intersection with the x-axis at

low frequencies. It has to be noticed that the lower limit of the frequency range for EIS was set to 1 Hz for "ageing tests" which can be a quite high value compared to transport phenomenon time constant which have been later observed as being as high as a few seconds or a few tenth of second. This means that $R_{ohm} + R_{elec}$ may not always correspond to the total polarization resistance which then may be under-estimated.

A third contribution at low frequency (0.6 Hz) which is often ascribed to mass transport phenomenon at the cathode side appears in some cases [28]. This contribution will be called "low frequency arc" and discussed more deeply below.

It is important to keep in mind that these analyses are based on a macroscopic measurement corresponding to an overall behaviour, therefore giving a response averaged over the whole fuel cell. From this point of view the cell seems to operate in a homogeneous way. However, fuel cell operation is very heterogeneous by nature, due to the strong influence of MEA hydration extent on the transport properties and electrochemical phenomena. Water concentration variations can be found both between anode and cathode sides (through the membrane thickness) and between gas inlets and outlets (on the membrane plane). The last point is especially true for our setup where dry gases are supplied in a co-flow configuration.

2.5. Water collection

During fuel cell operation water was regularly collected at both electrode sides.

As the fuel cell was operated at a constant current, identical for all the tests, the total quantity of produced water has to be the same whatever the stoichiometry. The Faradaic efficiency of the electrochemical reactions (especially the four electrons reduction of oxygen into water) was supposed to be the same in each case and equal to one. The theoretical amount of produced water per hour was therefore calculated as follows:

The quantity (mol) of electrons n_e flowing through the external circuit at an intensity I in the fuel cell during Δt is:

$$n_e = \frac{I \cdot \Delta t}{N_a \cdot e} \tag{2}$$

Considering the reaction at cathode side $O_2 + 4H^+ + 4e^- \rightarrow 2H_2O$, the corresponding molar quantity of H_2O is

$$n_{H_2O} = \frac{n_e}{2} \tag{3}$$

So the quantity of water produced by the fuel cell over time is given by

$$\frac{m_{H_2O}}{\Delta t} = \frac{1}{2} \cdot \frac{I}{N_a \cdot e} \cdot M_{H_2O} \tag{4}$$

with $I = 2$ A, $N_a = 6.02 \times 10^{23}$ mol^{-1}; $e = 1.602 \times 10^{-19}$ C; $M_{H_2O} = 18$ g mol^{-1} giving $m_{H_2O}/\Delta t = 0.67$ g h^{-1}.

At the exit of the fuel cell, water was condensed at room temperature and weighed. In general the quantity of water collected in the condensers was underestimated. Indeed, water was condensed at room temperature, which means that some water still in vapour phase was not collected. We can calculate this quantity of water for each gas stoichiometry condition as explained below.

In the phase separator, H_2O partial pressure is equal to H_2O saturation vapour pressure at room temperature:

$$P_{H_2O} = P_{satvap}(T_{amb}) = \frac{n_{H_2O}}{n_{gas} + n_{H_2O}} \cdot P_{tot} \tag{5}$$

where $P_{satvap}(T_{amb}) = 31.7$ mbar and $P_{tot} = 2$ bar (total pressure in the phase separator). n_{H_2O} is the molar flow of H_2O and n_{gas} is the molar flow of gas at the exit of the bench (difference between flow of gas at the inlet and consumed gas by the reactions).

Table 2
Uncondensed water flows at both bench outlets.

Gas	Stoichiometry	Flow of non condensed water (mg h^{-1})
H_2	1.5	5.4
H_2	3	22
O_2	1.5	2.7
O_2	3	11

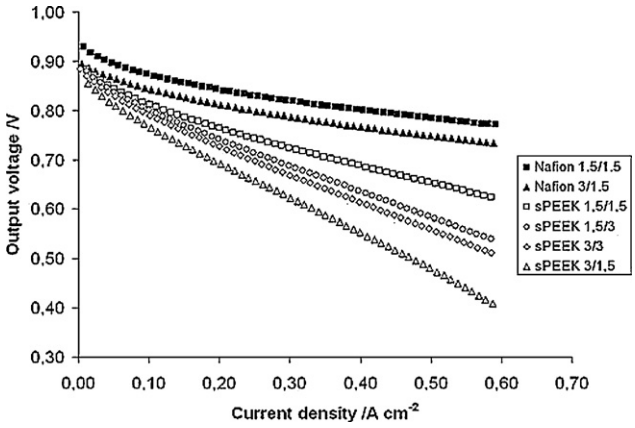

Fig. 3. Polarization curves after 10 h of operation for different stoichiometric coefficients.

Therefore, for both cathode and anode sides at the two tested stoichiometries, the quantity of uncondensed water vapour is summarized in the following table (Table 2):

All the below reported collected water will include this calculated amount of uncondensed water.

As we measured the amount of collected water, we calculated the molar flow of water at both electrode sides. Knowing P_{H_2O} from Eq. (5), relative humidity at the outlet of gases was calculated with

$$\text{RH} \quad (\%) = \frac{100 \cdot P_{H_2O}}{P_{vapsat}(80\,^\circ\text{C})} \tag{6}$$

where $P_{vapsat}(80\,^\circ\text{C}) = 450$ mbar.

3. Results and discussion

3.1. Influence of gas stoichiometry on fuel cell performances: characterizations at the beginning of the test

The polarization curves have been drawn after 10 h of test for the different operating conditions (Fig. 3). Values at OCV and 0.4 A cm^{-2} are summarized in Table 3.

A slight decrease of the OCV value from 904 to 882 mV is observed for sPEEK respectively for 1.5/1.5 and 3/1.5 stoichiometries. For Nafion, a larger OCV decrease from 940 mV (1.5/1.5) to 902 mV (3/1.5) is observed. This decrease of OCV can be attributed to H_2 permeation. At OCV, gases are not consumed and a small amount of hydrogen crosses the membrane and is oxidized at the cathode, resulting in a parasitic reaction which lowers the potential

Table 3
OCV values and cell voltage at 0.4 A cm^{-2} depending on gas stoichiometry for both sPEEK and Nafion membranes.

	sPEEK			Nafion		
Stoichiometry anode/cathode	1.5/1.5	1.5/3	3/3	3/1.5	1.5/1.5	3/1.5
OCV (mV)	904	900	886	882	940	902
Cell voltage at 0.4 A cm^{-2} (mV)	690	640	610	550	800	770

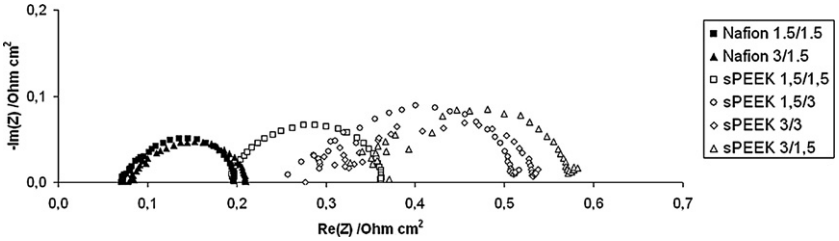

Fig. 4. EIS after 10 h of operation for different gas stoichiometries both for Nafion and sPEEK membranes.

measured at the cathode [29–31]. This effect is not observed with O_2 stoichiometry, as O_2 permeation in Nafion is three times lower than H_2 permeation according to Takaichi et al. [32].

Stoichiometry impact on initial performance (after 12 h of equilibrium and 10 h of operation) appears when comparing the cell voltage at 0.4 A cm^{-2} after 10 h of test. For sPEEK, the cell voltage decreases from 690 to 550 mV at 0.4 A cm^{-2} for 1.5/1.5 and 3/1.5 respectively (Table 3). This loss is usually correlated to the increase of the ionomer resistivity both in the membrane and the electrodes [33]. Such an increase of the ionomer resistivity can be observed when the ionomer is drying. Therefore, the drier the ionomer is, the lower the performance. Indeed, since we used dry gases, the higher the stoichiometry (meaning the higher the gas flows), the drier ionomer. However, the fact that we observe better performance with 3/3 compared to 3/1.5 stoichiometry requires a deeper analysis than just simple considerations on the average hydration of the ionomer. In the case of Nafion the cell voltage is 800 and 770 mV at 0.4 A cm^{-2} for 1.5/1.5 and 3/1.5 respectively. This can be attributed to ionomer drying but also to H_2 permeation which is already responsible for a loss of OCV values (−38 mV). EIS have been recorded to have a deeper analysis (Fig. 4).

EIS have been analysed by considering that R_{ohm} is mainly ascribed to proton transport within the membrane. R_{elec} is ascribed to physical phenomenon like charge/mass transfer or proton migration occurring within the electrodes (cf. Section 2).

The lower the performance the noisier the spectra are at high frequency. This may be ascribed to the amplitude of the current perturbation during EIS analysis, which is too high. The response of the system is too slow compared to the applied perturbation and is then non linear.

However, the ohmic losses are confirmed by EIS measurements which show a significant shift of the spectra to higher values when gas stoichiometry is increased. R_{ohm} and R_{elec} values for both sPEEK and Nafion membranes are reported in Table 4. For sPEEK, the shift of R_{ohm} between 1.5/1.5 and 3/1.5 configurations corresponds to a decrease of the ionomer averaged conductivity from 31 to 16 mS cm^{-1}. With Nafion, R_{ohm} is shifted from 0.07 (1.5/1.5) to 0.08 Ω cm^2 (3/1.5) which corresponds to a conductivity shift from 125 to 100 mS cm^{-1}, respectively. Gas stoichiometry has no clear impact on R_{elec}, but R_{elec} increases when moving from Nafion to sPEEK membrane. This can have two different origins:

- The electrode–membrane interface is of poor quality (assembly of a nonperfluorinated membrane with a Nafion coated electrode) [34].
- The membrane water transport properties have an impact on the electrodes behaviour as they result into dry or more hydrated areas.

From these values a direct correlation between operating conditions and R_{ohm} for sPEEK membranes is clearly observed. An increase of R_{ohm} can be attributed to a lower global hydration of the membrane, even if this hydration can be very heterogeneous. To evaluate the overall ionomer hydration, water was collected on both electrode sides (reminder: we used dry gases, and water is produced only at the cathode, but some water was collected at the anode side, due to the back-diffusion effect). The amount of collected water was used to calculate the RH at the gas outlet of both electrodes using Eqs. (5) and (6) as already stated in Section 2.

Table 4 presents the amount of water collected at the anode (the rest being collected at the cathode), the total flow of produced water, the corresponding RH on both sides and R_{ohm} and R_{elec} values, and this for different gas stoichiometries. It first appears that, contrary to what is often thought, a higher quantity of collected water at an electrode side does reflect a better hydration of this electrode. Indeed for sPEEK 1.5/1.5 stoichiometry, 19% of produced water (0.70 g h^{-1}) is collected at the anode, giving 100%RH at the gas outlet, whereas for 3/3 configuration, 43% of produced water (0.77 g h^{-1}) is collected at the anode but RH at the outlet of this electrode is only 79%.

3.1.1. sPEEK results

First, for all the studied stoichiometries a higher amount of water is collected at the cathode than at the anode side. Calculations show that MEA is more hydrated at the cathode side than at the anode side. As water is produced at the cathode, no matter the operating conditions, this electrode will be the most hydrated one. Variations of the collected water distribution between anode and cathode are probably due to an evolution of water concentration gradients across the membrane and along the flow field channels (gases are dry at the inlet but they become hydrated or even saturated at the outlet) depending on operating conditions. This variation of water distribution has a direct impact on fuel cell performance.

Table 4
Collected water, calculated RH at both sides and R_{ohm} and R_{elec}, for different gas stoichiometry, both for Nafion and sPEEK membranes.

	sPEEK				Nafion		Theory
Gas stoichiometry anode/cathode	1.5/1.5	1.5/3	3/3	3/1.5	1.5/1.5	3/1.5	All
Fraction of total water amount collected at the anode	19%	16%	43%	34%	39%	60%	–
Flow of collected water (g h^{-1})	0.70	0.65	0.77	0.69	0.69	0.77	0.67
Calculated %RH at the outlet of anode/cathode	sat/sat	sat/sat	79/sat	65/sat	sat/sat	sat/sat	–
R_{ohm} (Ω cm^2)	0.19	0.26	0.32	0.35	0.07	0.08	–
R_{elec} (Ω cm^2)	0.17	0.25	0.21	0.23	0.12	0.12	–

"sat" means the gas is saturated with presence of liquid water.

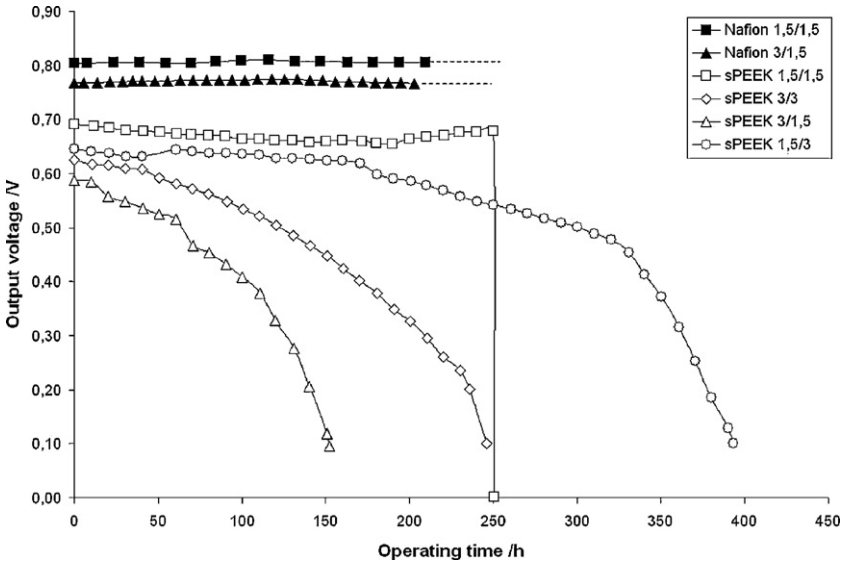

Fig. 5. Evolution of output voltage for different gas stoichiometry configurations.

3.1.1.1. Increase of stoichiometry at the cathode side. When stoichiometry is increased only at the cathode side (i.e. from 1.5/1.5 to 1.5/3), a slight decrease of collected water at the anode is measured, going from 19% to 16% of the total amount of water (respectively 0.70 and 0.65 g h^{-1} for 1.5/1.5 and 1.5/3 configurations). According to calculations, gases become totally saturated at the outlet at both electrode sides. However, as relative humidity at gas outlets depends on both quantities of collected water and gas flow rates, we assume that the average humidity on both sides is decreased in the 1.5/3 configuration. This local drying can participate to the loss of performance observed in Table 3: output voltage is decreased from 690 to 640 mV at 0.4 A cm^{-2}.

3.1.1.2. Increase of stoichiometry at the anode side. When stoichiometry is increased only at the anode side (i.e. from 1.5/1.5 to 3/1.5), impact on water management is more pronounced than at the cathode side as water collected at the anode increases from 19% (of 0.70 g h^{-1}) to 34% (of 0.69 g h^{-1}). As the flow of dry gas is doubled at the anode, a local but huge drying (relative humidity drops from saturation to 65% at the anode when stoichiometry is increased from 1.5 to 3) can be responsible for the observed loss of performance (from 690 to 550 mV at 0.4 A cm^{-2}).

3.1.1.3. Increase of stoichiometry at both electrode sides. The highest amount of water collected at the anode is reached for the stoichiometry 3/3 with 43% of the total water amount (0.77 g h^{-1}). Additional information is given by the total amount of collected water (anode + cathode) per hour. In 1.5/1.5, 1.5/3, 3/1.5 configurations, collected water is close to theory. The little gap can be due to the bad precision of the bench for controlling the current. However, there is a huge difference between the 3/3 test and theory with a total amount of collected water per hour of 0.77 g h^{-1}, about 15% more than theoretically expected. This implies a water production without any electron involved, as a constant current was generated. Therefore only gas crossover can explain such an observation, and we know that crossover of both gases to form H_2O can happen if they are in sufficient stoichiometry [35,36]. This excess of produced water for 3/3 stoichiometries results into better hydration of the membrane and thus better performance (610 mV vs. 550 mV for 3/1.5).

3.1.2. Nafion results

As a comparison, tests with Nafion for 1.5/1.5 and 3/1.5 stoichiometries have been performed. These stoichiometries correspond to the best and the worst performing situations, respectively, for sPEEK. Whatever the stoichiometry studied, Nafion performs better than sPEEK. This can be explained by both lower R_{ohm} and R_{elec} with Nafion (around 0.07 and 0.12 Ω cm^2 respectively vs. 0.19 and 0.17 Ω cm^2 for sPEEK in 1.5/1.5). The lower R_{ohm} for Nafion comes from its better proton conductivity; however the lower R_{elec} appears at first sight somehow surprising as electrodes are the same for both Nafion and sPEEK MEAs. As seen before in literature [34], this difference between Nafion and other kind of membrane can be ascribed to the quality of the membrane–electrode interface which is expected to be lower with hydrocarbon membrane. However, an additional explanation of the lower R_{elec} measured for Nafion can be a better water distribution within the MEA for Nafion than for sPEEK, along with a better hydration and therefore performance of both electrodes.

Collected water amounts at 3/1.5 stoichiometries for sPEEK and Nafion highlight the very different behaviour of the two membranes. For Nafion, 60% of the water is collected at the anode side, whereas for sPEEK only 36% of the water is collected at this side. Therefore, with Nafion, back-diffusion process is more efficient than electro-osmosis, and a lot of water is going from cathode to anode. As shown by Kreuer [37], water transport properties are totally different between Nafion and poly-aromatic membranes. He studied sPEEKK, which structure is close to sPEEK in terms of chemical and mechanical properties, and showed that in sPEEKK the hydrophilic network is composed of narrow and dead-end channels, whereas this network is larger and more defined for Nafion. Water is thus much more bounded to the polymer in sPEEKK membranes than it is in Nafion, which results into a water diffusion coefficient 10 times lower for sPEEKK than Nafion.

Collected water results for 3/1.5 stoichiometry show that more water is collected for Nafion (0.77 g h^{-1}) than what expected in theory (0.67 g h^{-1}), or for sPEEK in 3/1.5 (0.69 g h^{-1}). This can be ascribed to H_2 crossover that leads to water production without redox reactions. Comparisons of permeability between Nafion and poly-aromatics are very rare and quite complex as measurement techniques and parameters are numerous. However, H_2 crossover in Nafion is found to be 10 times higher than in sPEEK/PVDF (PolyVinyliDene Fluoride) blends [38] or twice higher than in Bi

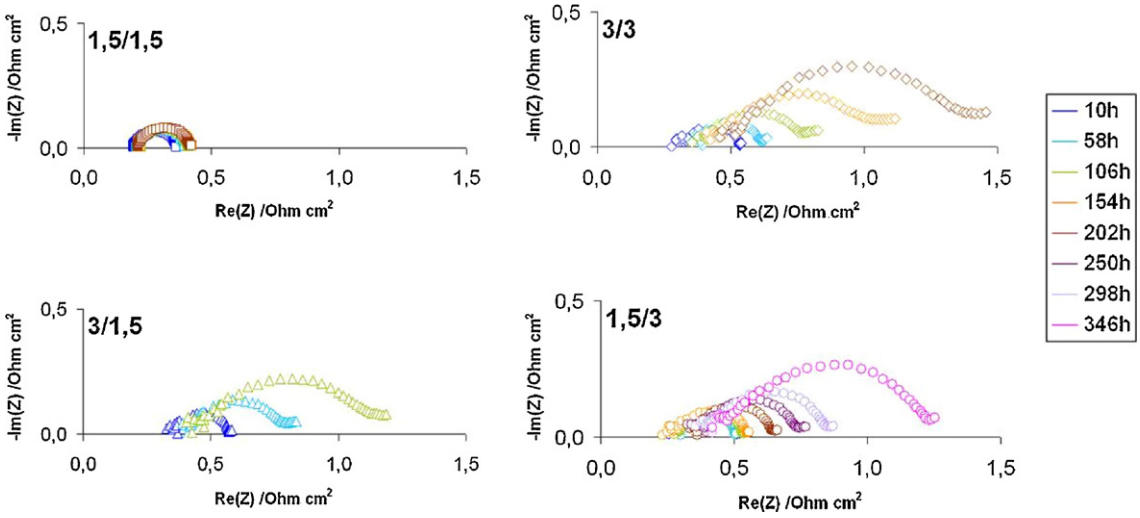

Fig. 6. Evolution of the EIS at 0.4 A cm^{-2} in dry gases for different gas stoichiometries for sPEEK.

Phenyl Sulfone H-form (BPSH) [13]. Also, many studies [32,39] have shown that in general ionomer membranes are more subject to gas permeation when hydrated. This can explain the difference of collected water in 3/1.5 between Nafion (0.77 g h^{-1}) and sPEEK (0.69 g h^{-1}). Indeed, as Nafion is more hydrated, gas permeability is increased, leading to more water production and better performance.

All these results show that an increase of stoichiometry can impact water distribution through the membrane and along the gas channels, and therefore fuel cell performance which hence depends on both operating conditions and membrane intrinsic properties. The evolution of this water distribution during membrane lifespan is studied in the next part.

3.2. Impact of gas stoichiometry on the fuel cell performance: lifespan evolution

The performance for each test is presented in Fig. 5 as the evolution of the output voltage as a function of time, with a current density set to 0.4 A cm^{-2}.

Whatever the stoichiometry, output voltage for sPEEK membrane is found to be lower than for Nafion. Interestingly, for sPEEK the lower the initial performance the faster it decreases. sPEEK, 1.5/1.5 test showed a quite stable output voltage (around 0.69 V) until the sudden shutdown of the cell after 250 h. For this specific case we assume that a sudden defect in gas supply could be responsible for the early crash of the cell. A progressive drop of performance is observed for sPEEK for the other gas stoichiometries. The sharper drop of performance is observed for the stoichiometry 3/1.5, which lasted only 150 h; then comes the 3/3 stoichiometry which lasted 250 h and finally the 1.5/3 stoichiometry which lasted almost 400 h with a very slow drop of performance for the first 200 h. All cells were disassembled after shutdown, to check for membrane perforation. However no such damage was observed even for 1.5/1.5 (cell abrupt failure). Concerning Nafion, gas stoichiometry was not observed to have any strong effect on the performance evolution.

In order to understand more accurately the behaviour of the cells over time, EIS measurements were done regularly.

EIS measurements evolution with time is presented in Fig. 6 for the four stoichiometries tested with sPEEK membrane. Evolution of R_{ohm} and R_{elec} as a function of time for both sPEEK and Nafion is presented in Fig. 7.

From these data we can observe a general trend for sPEEK with an increase of both R_{ohm} and R_{elec} through operating time, however very limited for the 1.5/1.5 stoichiometry. These phenomena can be correlated to each other and are largely enhanced as stoichiometry is increased whatever the electrode side. The increase of R_{ohm} values can be associated with an average drying of the ionomer with time. As R_{elec} values increase even more than R_{ohm} ones, this suggests changes at the electrodes that impact the performance. For Nafion, R_{ohm} and R_{elec} are constant through time, which correlates with the constant performance observed.

It should be noticed that water was always collected at a constant rate at the exit of the cell (Fig. 8). Therefore, even though at the beginning of the test, performance depends on water distribution between anode and cathode, the decrease of performance over time seems to depend on other phenomena.

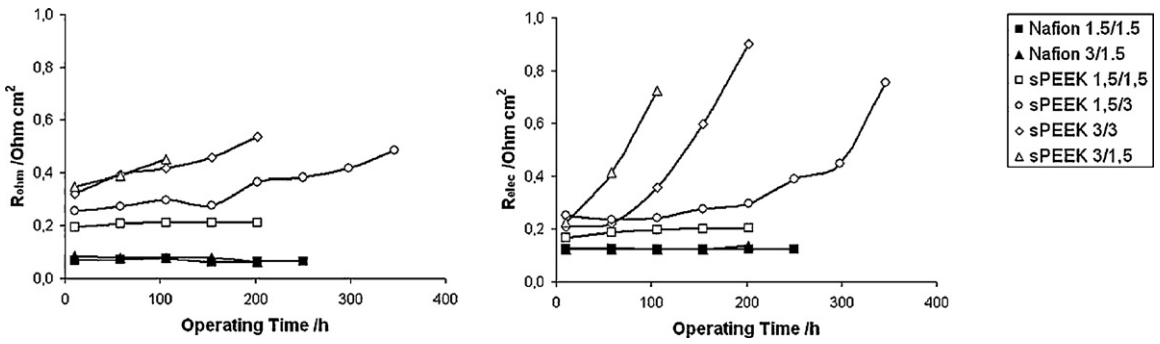

Fig. 7. Evolution of R_{ohm} and R_{elec} at 0.4 A cm^{-2} in dry gases for different gas stoichiometries for both sPEEK and Nafion.

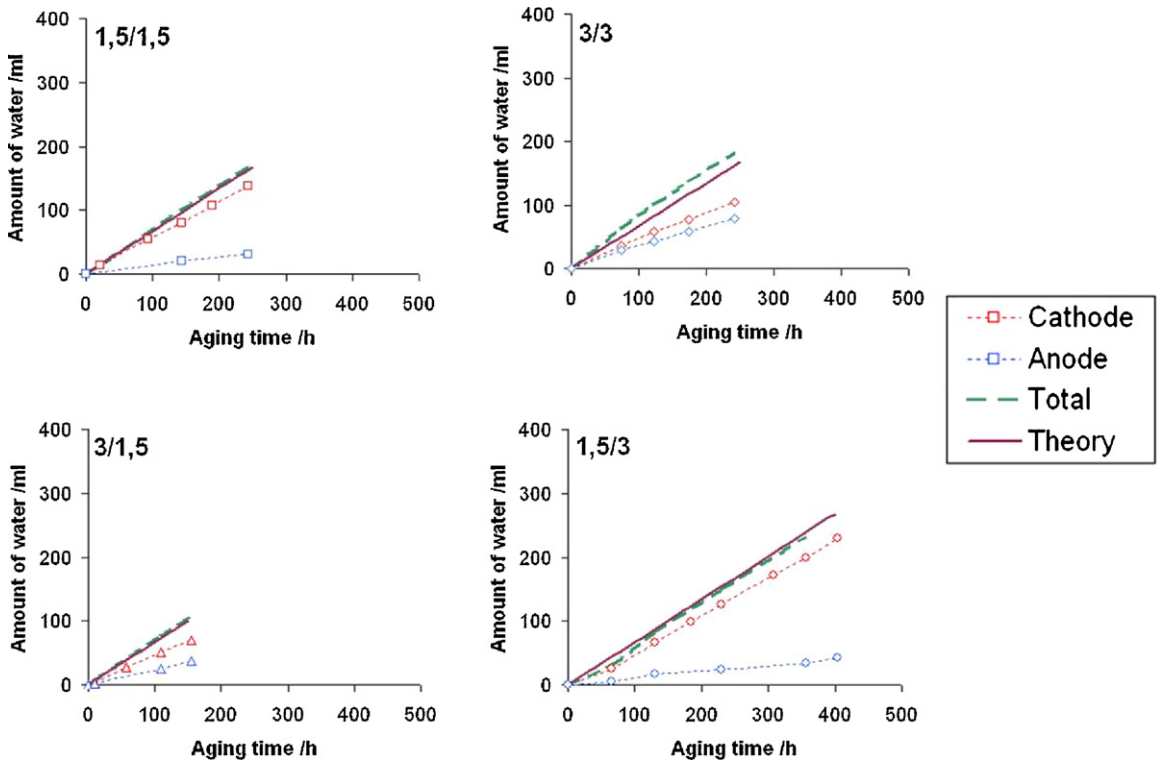

Fig. 8. Amount of collected water at the anode side (blue), cathode side (red), total (green) and theoretical (purple) amount of water for different stoichiometries. (For interpretation of the references to color in this figure legend, the reader is referred to the web version of the article.)

We assume that the observed decrease of performance over time is mainly related to the evolution of water distribution in the flow field (not between anode and cathode but between gas inlet and outlet). Even if hydration of the flow field channels is already clearly heterogeneous at the beginning of the tests, the large increase of R_{elec} observed over time suggests that this heterogeneity gets stronger with time leading to an important drying of the inlets (more pronounced at the anode). To correlate more accurately the behaviour of R_{elec} to the dryness of an electrode, short tests have been performed on sPEEK at two different RH (9% and 100%), at very high gas flow rate (to homogenize working conditions at inlet and outlet).

Impact of drying electrodes on EIS was observed by comparing two extreme conditions: 100%RH at both anode and cathode (wet gases) and 9%RH on both electrodes (dry gases). The evolution of EIS at 100/100%RH and 9/9%RH for different current densities is presented in Fig. 9.

In both cases, spectra are noisy at low frequencies (<10 Hz). This can be due to inductive phenomena associated with mass and/or charge transfer at the cathode side [40]. This noise decreases when current density is increased.

If RH is set to 100% on both electrode sides, R_{ohm} remains stable with a value of 0.14 $\Omega\,cm^2$ which corresponds to a conductivity of 45 $mS\,cm^{-1}$. This indicates a homogeneous water repartition which does not evolve with current density. However, R_{elec} decreases from 0.61 to 0.08 $\Omega\,cm^2$ for 0.1 $A\,cm^{-2}$ and 0.8 $A\,cm^{-2}$ respectively. As mentioned in literature, this is due to a faster charge transfer as the current density increases.

If RH is set to 9% on both sides, R_{ohm} decreases from 0.72 to 0.68 $\Omega\,cm^2$ when current density is increased from 0.1 to 0.2 $A\,cm^{-2}$. This is due to the increase of average RH and better hydration of the ionomer as the cell produces more water (higher current densities). If current density is increased to 0.4 $A\,cm^{-2}$, R_{ohm} increases while the low frequency arc (0.6 Hz) appears. The increase

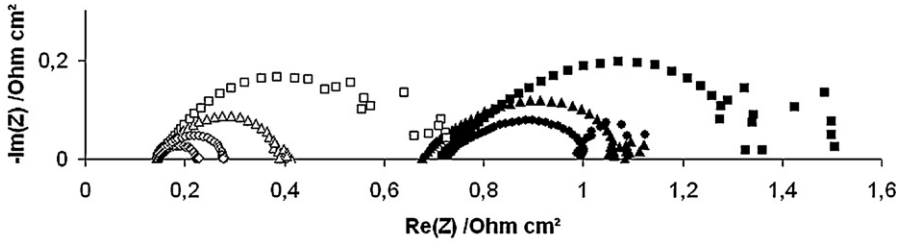

100/100%RH				
Current density (A cm⁻²)	□ 0.1	△ 0.2	◇ 0.4	◇ 0.8
R_{ohm} (Ω cm²)	0.14	0.14	0.14	0.15
R_{elec} (Ω cm²)	0.61	0.26	0.14	0.08
Additional contribution (<0.5Hz) ?	N	N	N	N

9/9%RH			
Current density (A cm⁻²)	■ 0.1	▲ 0.2	● 0.4
R_{ohm} (Ω cm²)	0.72	0.68	0.73
R_{elec} (Ω cm²)	0.72	0.39	0.27
Additional contribution (<0.5Hz) ?	N	N	Y

Fig. 9. EIS for two operating conditions: 100/100%RH (white) and 9/9%RH (black) and for different current density.

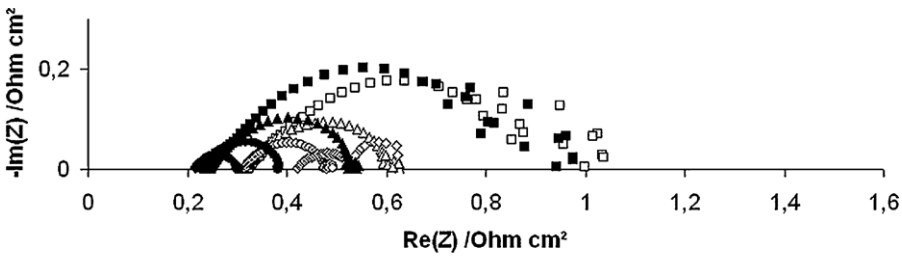

100/0%RH					0/100%RH				
Current density (A cm⁻²)	■ 0.1	▲ 0.2	● 0.4	◆ 0.8	Current density (A cm⁻²)	□ 0.1	△ 0.2	◇ 0.4	◇ 0.8
R_{ohm} (Ω cm²)	0.25	0.24	0.23	0.22	R_{ohm} (Ω cm²)	0.32	0.31	0.31	0.42
R_{elec} (Ω cm²)	0.75	0.30	0.15	0.08	R_{elec} (Ω cm²)	0.72	0.29	0.17	0.11
Additional contribution (<0.5Hz) ?	N	N	N	N	Additional contribution (<0.5Hz) ?	N	N	N	Y

Fig. 10. EIS for two operating conditions: 100/0%RH (black) and 0/100%RH (white) and varying current density.

of R_{ohm} and the appearance of the low frequency arc seem to be correlated and could be due to the drying of ionomer in the active layer. Indeed, an increase of current density emphasizes electro-osmosis and dries the anode side [27].

The effect of drying anode or cathode side is studied by comparing the EIS obtained at 100/0%RH and 0/100%RH (Fig. 10).

In the 100/0%RH configuration, R_{ohm} slightly decreases (from 0.25 to 0.22 Ω cm²) if current density is increased, which is due to better hydration with higher water production. R_{elec} continuously strongly decreases when current density increases, a behaviour similar to what was found for the 100/100%RH case. However at 0.1 A cm^{-2}, R_{elec} is higher for 100/0%RH (0.75 Ω cm²) than for 100/100%RH (0.61 Ω cm²). This shows that ionomer hydration at the cathodic active layer has an influence on electrode behaviour (cathode) that could be due to migration of protons within the active layer.

The 0/100%RH configuration is similar to the 100/0%RH one at low current densities (from 0.1 to 0.4 A cm^{-2}). R_{ohm} remains stable around 0.31 Ω cm² and is higher than R_{ohm} values obtained for 100/0%RH. This shows a higher impact of dry gas at the inlet of anode side (where no water is produced) than at the cathode side. For higher current density (0.8 A cm^{-2}) R_{ohm} is shifted to higher values (0.42 Ω cm²) and a low frequency arc (0.6 Hz) appears, similar to what observed for the 9/9%RH case. Thus this contribution is ascribed to ionomer drying at the anode. If current density is increased to 1.0 A cm^{-2} (Fig. 11), R_{ohm} values keep on increasing and R_{elec} starts to increase while the low frequency arc becomes stronger. This shows that there is an important drying of the ionomer that can be due to a low back-diffusion. At high current density, electro-osmosis can induce an important flow from anode to cathode, not compensated by back-diffusion. The extreme case would be a net flow from anode to cathode which totally dries out the ionomer at the anode.

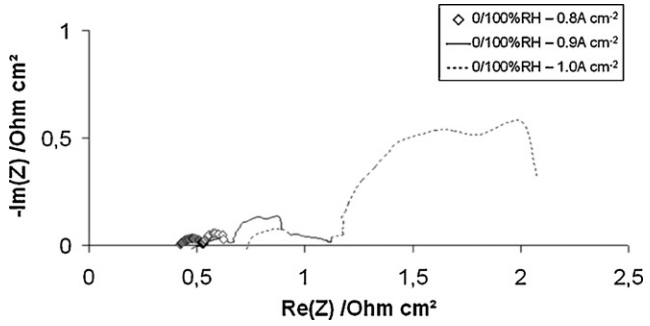

Fig. 11. Impact of high current densities on EIS at 0/100%RH.

All these "hydration tests" show that using dry gases at high flow rate leads to

- an increase of R_{ohm} due to the drying of the ionomer, but also
- an increase of R_{elec} which is generally ascribed to bad charge or mass transfer. However, we propose here to associate the R_{elec} increase to the drying of the ionomer especially at the anode, which limits protons migration within the active layer, and leads to the appearance of the low frequency arc.

This last EIS behaviour is often explained by a flooding at the cathode [41–43] but this is rather unlikely because of the high values of P_{O_2} and flow rate used here. Moreover if gas flows are reduced to 50 N ml min^{-1} in order to favour flooding, no change is observed on EIS.

These experiments clarify the EIS evolution which was observed during sPEEK "ageing tests". As shown before, the increase of stoichiometry from 1.5 to 3 whatever the electrode side was followed by a little increase of R_{ohm} and a large increase of R_{elec}, as well as the appearance of a low frequency arc. These MEAs behaved like dehydrated MEAs on which the current density was increased with time. However, during "ageing tests" current density was constant. We then assume that some areas are getting dryer while others are getting more hydrated with time. It has already been shown that on both electrode sides current density, temperature [44,45] and hydration [46] can vary along the channels going from the inlet to the outlet of the gases, which leads to a very heterogeneous system. Hence this evolution of R_{ohm}, R_{elec} and low frequency arc (0.6 Hz) can be interpreted on the basis of an increase of the inlet–outlet hydration heterogeneity, with a part of the MEA close to the inlet becoming dryer, whereas MEA close to the outlet becomes better hydrated. This phenomenon amplifies with time, as the local current density decreases at the dry inlet, making it even drier (no water being produced in this area, a phenomenon enhanced by the co-flow configuration). Since the total current density is constant, the local current density has to increase at the outlet, producing more and more water and amplifying this hydration heterogeneity in a vicious circle.

This evolution of R_{ohm} and R_{elec} during sPEEK "ageing tests" was not observed with Nafion. As mentioned before, this can be due to its better diffusion properties [37] which are responsible for better performances but also faster hydration kinetics which makes the membrane hydration much more homogeneous both through the membrane and along the flow field channels. Therefore the impact of stoichiometry on the initial and lifelong performance is very limited for this type of membrane.

4. Conclusion

Fuel cell tests have been performed on sPEEK and Nafion membranes using dry gases. To explain the impact of gas stoichiometry on water management and its effect on both initial and long term performance, global characterizations have been performed during fuel cell tests like polarization curves, EIS measurements, output voltage monitoring and water collection at both sides.

First, we found that a lot of water collected at an electrode side does not necessarily means that this electrode is well hydrated, as it also depends on the applied gas flow rate and pressure.

Second, whatever the configuration, sPEEK performance was lower than Nafion's one. It is partly due to the lower conductivity of sPEEK which in conjunction with the use of dry gases gives a higher ohmic resistance. However it has been shown by EIS that sPEEK and Nafion different performance can be related to polarization resistances other than ohmic. We understood that these performance differences come from the heterogeneous repartition of water in the channels and through the MEA, a phenomenon particularly pronounced for sPEEK membrane due to its lower water diffusion coefficient.

It has been shown that water distribution within the MEA can evolve during fuel cell operation, which in the case of sPEEK leads to a decrease of performance. This phenomenon is amplified by the use of dry gases and is observed through the increase of R_{ohm} and R_{elec}, and the appearance of low frequency arc on EIS, which were attributed to ionomer drying in the electrodes. This water distribution issue is amplified at the anode side and increases with time resulting into a drying phenomenon at the inlet and a higher hydration at the outlet. This drop of performance is not observed for Nafion, thanks to the faster hydration/dehydration kinetics of this polymer.

Therefore, to get better performance with alternative membrane, a good protonic conductivity is of course necessary, but, as demonstrated here, not enough. Intrinsic properties of the membranes and more particularly good water diffusion coefficient and hydration kinetics are also important to insure homogeneous water distribution in the MEA to get good electrode performances.

In this study MEA hydration distribution has been deduced from techniques giving only general information about water management. It would be challenging but certainly rewarding to get detailed hydration map of the MEA using local characterization techniques like direct optical visualization [47–49], X-ray [50] or neutron scattering [51].

References

[1] M. Reijalt, J. Clean. Prod. 18 (Suppl. 1) (2010) S112–S117.
[2] F.A. de Bruijn, V.A.T. Dam, G.J.M. Janssen, Fuel Cells 8 (1) (2008) 3–22.
[3] S.J. Peighambardoust, S. Rowshanzamir, M. Amjadi, Int. J. Hydrogen Energy 35 (17) (2010) 9349–9384.
[4] K.D. Kreuer, et al., Chem. Rev. 104 (10) (2004) 4637–4678.
[5] T.A. Zawodzinski, et al., J. Electrochem. Soc. 140 (4) (1993) 1041–1047.
[6] T.F. Fuller, J. Newman, J. Electrochem. Soc. 139 (5) (1992) 1332–1337.
[7] G. Alberti, et al., J. Membr. Sci. 185 (1) (2001) 73–81.
[8] Y. Paik, et al., Polymer 50 (12) (2009) 2664–2673.
[9] C. Perrot, et al., Polymer 50 (7) (2009) 1671–1681.
[10] C. Perrot, et al., J. Power Sources 195 (2) (2010) 493–502.
[11] G.M. Shashidhara, K.N. Kumar, Polym. Plast. Technol. Eng. 49 (8) (2010) 796–806.
[12] F. Piroux, E. Espuche, R. Mercier, J. Membr. Sci. 232 (1–2) (2004) 115–122.
[13] C.W. James Jr., et al., J. Membr. Sci. 309 (1–2) (2008) 141–145.
[14] C. Zhao, et al., J. Appl. Polym. Sci. 108 (1) (2008) 671–680.
[15] P. Xing, et al., J. Membr. Sci. 229 (1–2) (2004) 95–106.
[16] Q. Yan, H. Toghiani, H. Causey, J. Power Sources 161 (1) (2006) 492–502.
[17] A. Kazim, J. Power Sources 143 (1–2) (2005) 9–16.
[18] B. Wahdame, et al., Int. J. Hydrogen Energy 32 (17) (2007) 4523–4536.
[19] R. Jiang, H.R. Kunz, J.M. Fenton, J. Power Sources 150 (2005) 120–128.
[20] A. Turhan, et al., J. Power Sources 160 (2) (2006) 1195–1203.
[21] S. Qu, et al., J. Power Sources 185 (1) (2008) 302–310.
[22] S. Escribano, et al., J. Power Sources 156 (1) (2006) 8–13.
[23] I. Nitta, et al., J. Power Sources 171 (1) (2007) 26–36.
[24] J. Wu, et al., Int. J. Hydrogen Energy 33 (6) (2008) 1735–1746.
[25] T.E. Springer, et al., J. Electrochem. Soc. 143 (2) (1996) 587–599.
[26] M. Eikerling, A.A. Kornyshev, J. Electroanal. Chem. 475 (2) (1999) 107–123.
[27] V.A. Paganin, et al., Electrochim. Acta 43 (24) (1998) 3761–3766.
[28] N.H. Jalani, et al., J. Power Sources 160 (2) (2006) 1096–1103.
[29] C. Francia, et al., J. Power Sources 196 (4) (2010) 1833–1839.
[30] S.A. Vilekar, R. Datta, J. Power Sources 195 (8) (2009) 2241–2247.
[31] J. Zhang, et al., J. Power Sources 163 (1) (2006) 532–537.
[32] S. Takaichi, H. Uchida, M. Watanabe, Electrochem. Commun. 9 (8) (2007) 1975–1979.
[33] P. Kurzweil, H.J. Fischle, J. Power Sources 127 (1–2) (2004) 331–340.
[34] F. Lufrano, et al., J. Appl. Polym. Sci. 77 (6) (2000) 1250–1256.
[35] M. Gummalla, et al., J. Electrochem. Soc. 157 (11) (2010) B1542–B1548.
[36] J. Nam, et al., Appl. Energy 87 (12) (2010) 3699–3709.
[37] K.D. Kreuer, J. Membr. Sci. 185 (1) (2001) 29–39.
[38] T.Y. Inan, et al., Int. J. Hydrogen Energy 35 (21) (2010) 12038–12053.
[39] K. Broka, P. Ekdunge, J. Appl. Electrochem. 27 (2) (1997) 117–123.
[40] B.E. Conway, et al., Modern Aspects of Electrochemistry, Springer, US, 2002, pp. 143–248.
[41] S. Rodat, et al., J. Appl. Electrochem. 40 (5) (2010) 911–920.
[42] J.-M.L. Canut, R.M. Abouatallah, D.A. Harrington, J. Electrochem. Soc. 153 (5) (2006) A857–A864.
[43] T.J.P. Freire, E.R. Gonzalez, J. Electroanal. Chem. 503 (1–2) (2001) 57–68.
[44] K.-S. Choi, H.-M. Kim, S.-M. Moon, Int. J. Hydrogen Energy 36 (2) (2010) 1613–1627.
[45] I. Alaefour, et al., Electrochim. Acta 56 (5) (2010) 2591–2598.
[46] J.M. Sierra, J. Moreira, P.J. Sebastian, J. Power Sources 196 (11) (2011) 5070–5076.
[47] K. Tüber, D. Pócza, C. Hebling, J. Power Sources 124 (2) (2003) 403–414.
[48] S. Ge, C.-Y. Wang, J. Electrochem. Soc. 154 (10) (2007) B998–B1005.
[49] X.G. Yang, et al., Electrochem. Solid-State Lett. 7 (11) (2004) A408–A411.
[50] T. Mukaide, et al., J. Synchrotron Radiat. 15 (4) (2008) 329–334.
[51] A. Morin, et al., Int. J. Hydrogen Energy 36 (4) (2010) 3096–3109.